

# An investigation of the effect of powder on the impact characteristics between a ball and a plate using free falling experiments

H. Huang<sup>a</sup>, M.P. Dallimore<sup>a</sup>, J. Pan<sup>b,\*</sup>, P.G. McCormick<sup>a</sup>

<sup>a</sup> *Special Research Centre for Advanced Minerals and Materials Processing, University of Western Australia, Nedlands, WA 6907, Australia*

<sup>b</sup> *Department of Mechanical and Materials Engineering, University of Western Australia, Nedlands, WA 6907, Australia*

Received 13 January 1997; received in revised form 20 May 1997

## Abstract

The study of the mechanisms of mechanical alloying requires knowledge of the impact characteristics between the ball and vial in the presence of milling powders. In this paper, free falling experiments have been used to investigate the characteristics of impact events involved in mechanical milling. The effects of milling conditions, including impact velocity, ball size and powder thickness, on the coefficient of restitution and impact force are studied. It is found that the powder has a significant influence on the impact process due to its porous structure. This effect can be demonstrated using a modified Kelvin model. This study also confirms that the impact force is a relevant parameter for characterising the impact event due to its sensitivity to the milling conditions. © 1998 Elsevier Science S.A.

*Keywords:* Mechanical alloying; Microstructure; Milling

## 1. Introduction

The application of mechanical alloying has attracted considerable attention due to its versatility and robustness as a processing method for the synthesis of a wide range of materials, such as dispersion strengthened superalloys, nanophase materials, intermetallics and ceramics [1,2]. In recent years, extensive studies of the dynamics of the mechanical alloying process and their influence on microstructural changes of milled materials have emerged [3–11]. These studies have revealed that the reaction paths and end products of the mechanical alloying process are dependent on the physical and mechanical properties of the materials being milled and the type of milling process being employed. A given milling process can often be described in terms of the values of important process parameters. Among the important process parameters, the energy or power consumed during milling has been the focus of studies of milling dynamics [4–11].

In our previous work [12,13], a laboratory vibratory mill was developed for studying the relationship of the energy of individual collision events and the microstructural evolution of 304 stainless steel powder during milling. The vibratory mill [12] consisted of a vial containing a single ball subjected to a sinusoidal motion in the vertical direction. Due to the vertical constraint imposed on the ball, the collisions involved in the vibratory milling were characterised by normal impacts between a ball and a plate [12]. It was found that impact force is a suitable process parameter for evaluation of energy consumption associated with each individual collision event. Therefore, a characterisation of the effect of milling conditions, including the impact velocity, ball size and powder thickness, on the impact force will improve the understanding of the dynamics of the mechanical alloying process and, thus, give an improved appreciation of the potential of the technique. However, it is difficult to quantify the effect of milling conditions on impact events due to the complexity of the milling process.

Impact phenomena between a ball and a block of material have been extensively studied [14–18]. The

\* Corresponding author. Tel.: +61 09 3803600; fax: +61 09 3801024.

coefficient of restitution [14,17,18], reflecting the capacity of the contacting bodies to recover from the impact and the extent of energy loss during impact, and the impact force [15,16,18], characterising the severity of impact, have been the focus of these studies. In recent years, measurements of the effect of low-velocity impact on composite laminates [19,20] have received considerable attention as a result of the rapid development of composite materials. The impact force associated with individual collision events was used as a scale parameter for impact response measurements [21]. The impact involved in the mechanical milling process has some similar characteristics with composite laminates, such as inelasticity of the impacted materials and low impact velocities. However, the impact mechanism involved in the collision events during mechanical milling is considered to be more complicated due to the presence of the powder. Currently, little is known about the effect of the presence of powder on impact characteristics [22]. Thus, it is of significance to systematically study impact phenomena during the mechanical milling process.

In this study, a free falling experiment, a close analogy to the individual collision events occurring in vibratory milling [12], has been used to investigate the impact characteristics between a ball and a plate coated with a layer of powder. The effect of milling conditions on the coefficient of restitution and impact force are measured. In order to improve our understanding of the influence of the powder on the impact process, a modified Kelvin model has been used to model coefficients of restitution and impact forces. The comparison between the measurement and modelling is also presented.

## 2. Experiments

The experimental rig used in the free falling experiments is schematically illustrated in Fig. 1. A grinding ball was released from a height,  $h_0$ , impacting upon 304 stainless steel powder particles located in a shallow recess in the hardened steel plate (1). It should be noted that since 304 stainless steel is a ductile material, the focus of this work is thus on powders that deform during ball/powder collisions. The as-received powder has an average particle size of approximately 5  $\mu\text{m}$ . The powder was levelled before each impact and the powder thickness was calculated according to the mass of the powder, the powder density and the cross-sectional area of the recess. A force transducer (3) was mounted between the two steel plates (1 and 4) with a small pre-load force. The steel plate (4) was rigidly mounted to the ground. The time history of the impact force was monitored by the force transducer with its signals downloaded to a computer. A sampling rate of 10 kHz

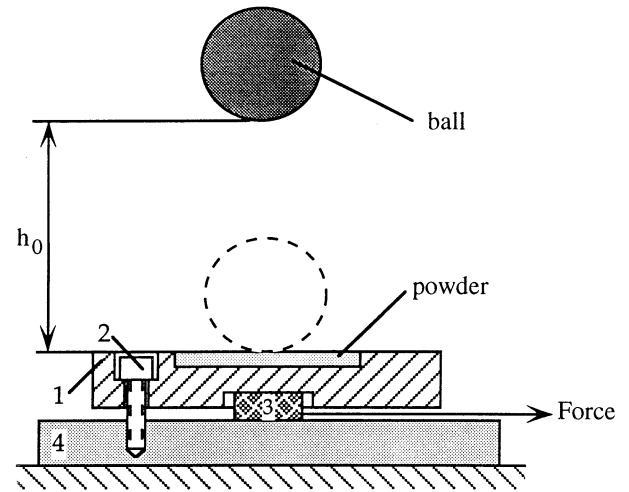


Fig. 1. The schematic of free falling experiment: (1) steel plate; (2) screws; (3) force transducer; and (4) steel base.

was used in order to obtain detailed information about the impact force (including the magnitude and duration). The time interval between the first two successive collisions,  $t_m$ , was obtained from the time history of the impact force shown in Fig. 2 and was used to determine the coefficient of restitution,  $e$ , by virtue of the impact relation [23]:

$$e = \left( \frac{g}{8h_0} \right)^{1/2} t_m \quad (1)$$

where  $g$  is the acceleration due to the earth's gravitation.

In the free falling experiments, the powder thickness was varied from 0 to 2.7 mm, which covers the range of powder thickness expected in the milling experiments [12]. Various ball diameters of 12.7, 15.9, 26, 31.8, 38.2 and 50 mm were used. The drop height of the ball was varied from 6 to 250 mm to obtain impact velocities of the same order as those found in the vibratory mill [12].

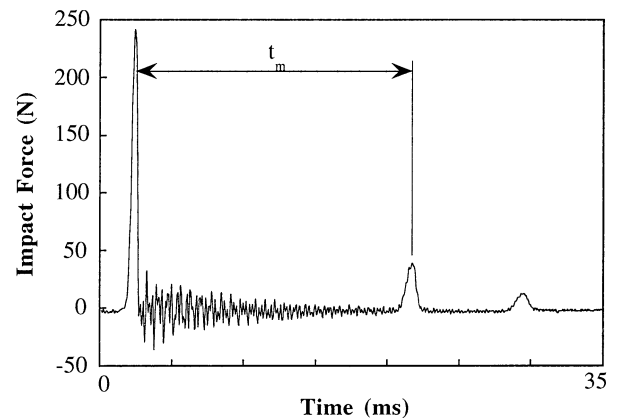


Fig. 2. Typical time history of the impact force during a free falling experiment.

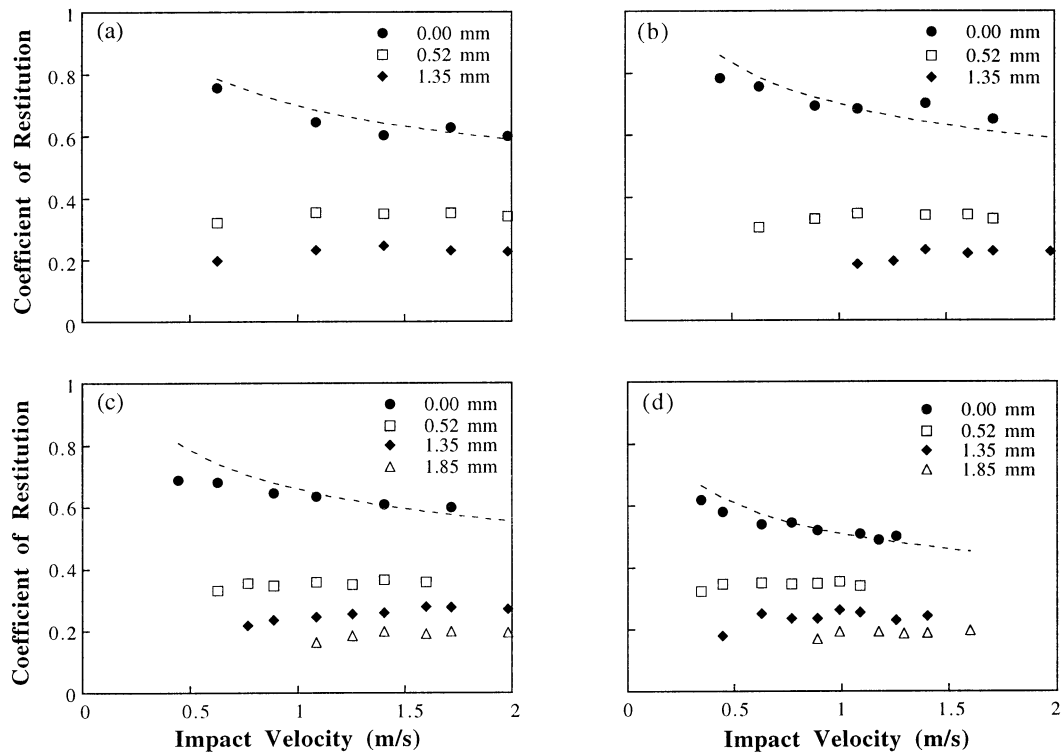


Fig. 3. Coefficient of restitution as a function of impact velocity for various ball sizes of: (a) 26 mm; (b) 31.8 mm; (c) 38.2 mm; and (d) 50 mm.

It is noted that in this study, for impacts where no powder is present, the ball was dropped on a 5 mm thick 304 stainless steel plate rigidly mounted in the shallow recess.

### 3. Results and discussion

#### 3.1. Coefficient of restitution

Measurements of the coefficient of restitution are plotted in Fig. 3 as a function of the impact velocity for different ball sizes and powder thicknesses. It is seen that for impacts where no powder is present,  $e$  decreases as the impact velocity increases. Previous studies [18] have shown that the impact of a ball on a plate is essentially elastic (or  $e$  is unity) until the normal impact velocity,  $v_n$ , exceeds a critical value causing plastic deformation. As the impact velocity is increased, the plastic deformation of the impacted material increases, thus resulting in a decrease in  $e$ . Previous experiments and theory [17,18] indicate that  $e$  for inelastic impacts varies as  $(v_n)^{-0.25}$ . In Fig. 3, curves of approximately  $(v_n)^{-0.25}$  ( $\cdots$ ) are also plotted to compare with the experimental measurements. The dependence of  $e$  on  $(v_n)^{-0.25}$  is reasonable for impacts without powder.

In Fig. 3, it can be observed that for impacts where powder is present,  $e$  initially increases slightly with increasing impact velocity before reaching a constant value at higher velocities. Similar behaviour has been reported by Liang et al. [22]. Evidently, when the powder is introduced to an impact zone, the effect of impact velocity on  $e$  is different from that for impacts where no powder is present. As Johnson [18] has discussed in relation to inelastic impacts,  $e$  is no longer solely related to the mechanical properties of the impacting objects, but now is dependent on the impact severity. At lower impact velocities, the existence of the powder significantly reduces the impact severity due to the interactions of powder particles before they are trapped by the impacting objects. This results in significantly reduced values of  $e$ . It should be noted that accurate values of  $e$  at very low velocities are difficult to obtain as small falling heights are required. When the impact velocity exceeded a critical velocity,  $e$  is more dependent on powder thickness than the impact velocity and ball size. As shown in Fig. 3,  $e$  reached a constant value at larger velocities. This also suggests that the measured value of  $e$  does not sensitively characterise the impact severity. To show the influence of the powder thickness, the maximum values of  $e$  in Fig. 3 are replotted in Fig. 4 as a function of initial powder thickness. It is seen that  $e$  decreased with the increasing powder thickness due to the increasing inelasticity of

the powder during impact. A detailed discussion of the effect of the powder will be given later.

### 3.2. Impact forces

Typical time histories of impact forces obtained from the free falling experiments are shown in Fig. 5. Fig. 5(a) shows impact forces corresponding to various impact velocities for a ball of 50 mm in diameter and a nominal powder thickness of 0.52 mm. Both the magnitude and duration of the impact force are influenced by the impact velocity. For large impact velocities, the corresponding impact forces exhibit narrow and high peaks, and for small impact velocities, flat and low peaks are observed. Fig. 5(b) shows the impact forces for various ball sizes for an impact velocity of 1.08 m s<sup>-1</sup> and a powder thickness of 0.52 mm. The larger ball sizes produce the wider and higher peaks. Fig. 5(c) shows the impact forces for various powder thickness for a ball diameter of 38.2 mm and an impact velocity of 1.08 m s<sup>-1</sup>. For the small powder thicknesses, the impact forces exhibit sharp and high peaks, and for the large powder thicknesses, they exhibit flat and low peaks. The results indicate that the impact velocity, ball size and powder thickness significantly influence impact force.

#### 3.2.1. Effect of impact velocity

The magnitude (i.e., the peak value) and duration of the impact force obtained from the free falling experiments are plotted in Fig. 6 as a function of the impact velocity for various powder thicknesses for two different ball sizes. For the powder thicknesses examined, the magnitude of the impact force increases (Fig. 6(a) and (c)), and the duration decreases (Fig. 6(b) and (d)), with the increasing impact velocity.

The data in Fig. 6 were fitted using the power law relationships:  $F \sim v^{n_1}$  and  $t \sim v^{n_2}$ , where  $F$  and  $t$  denote the magnitude and duration of the impact force,  $v$  is the

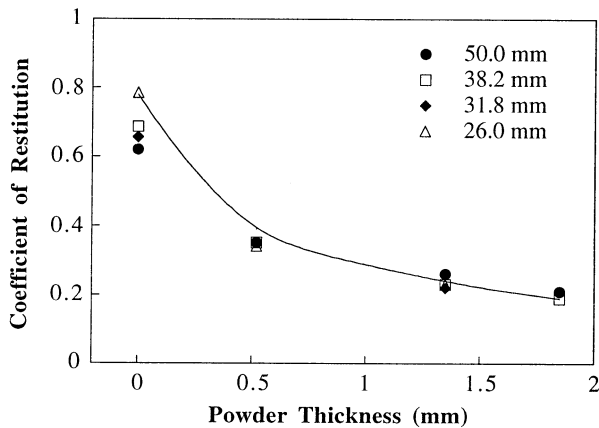


Fig. 4. Coefficient of restitution as a function of powder thickness.

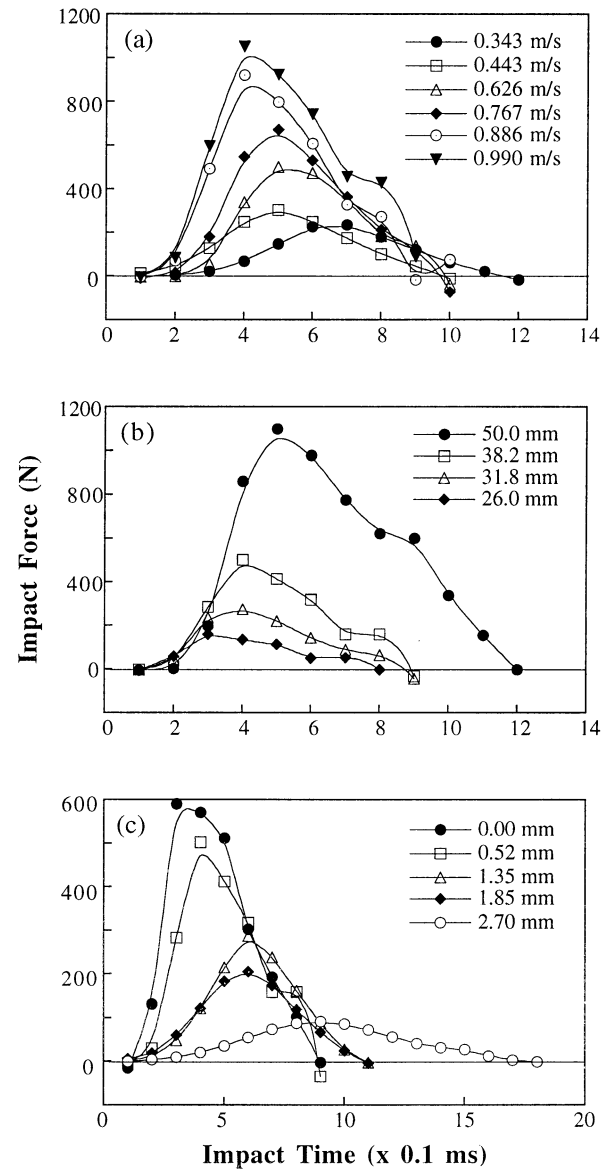


Fig. 5. Typical time histories of impact forces obtained from free falling experiments: (a) for various impact velocities, ball diameter 50 mm and powder thickness 0.52 mm; (b) for various ball sizes, powder thickness 0.52 mm and impact velocity 1.08 m s<sup>-1</sup>; (c) for various powder thicknesses, ball diameter 38.2 mm and impact velocity 1.08 m s<sup>-1</sup>.

impact velocity, and  $n_1$  and  $n_2$  are the indices representing the influence of the impact velocity. The results from the curve fitting are also illustrated in Fig. 6 (—). Values of  $n_1$  and  $n_2$  are given in Table 1. It is found that for impacts without powder, values of  $n_1$  for the 38.2 and 50 mm diameter balls are 1.53 and 1.42, and values of  $n_2$  are  $-0.23$  and  $-0.33$ , respectively. Hertz impact theory [15] shows that in the case of the impact between a ball and a plate, the relationship between the impact force and the impact velocity obeys a power law. The magnitude and duration of the impact force are represented as follows [15]:

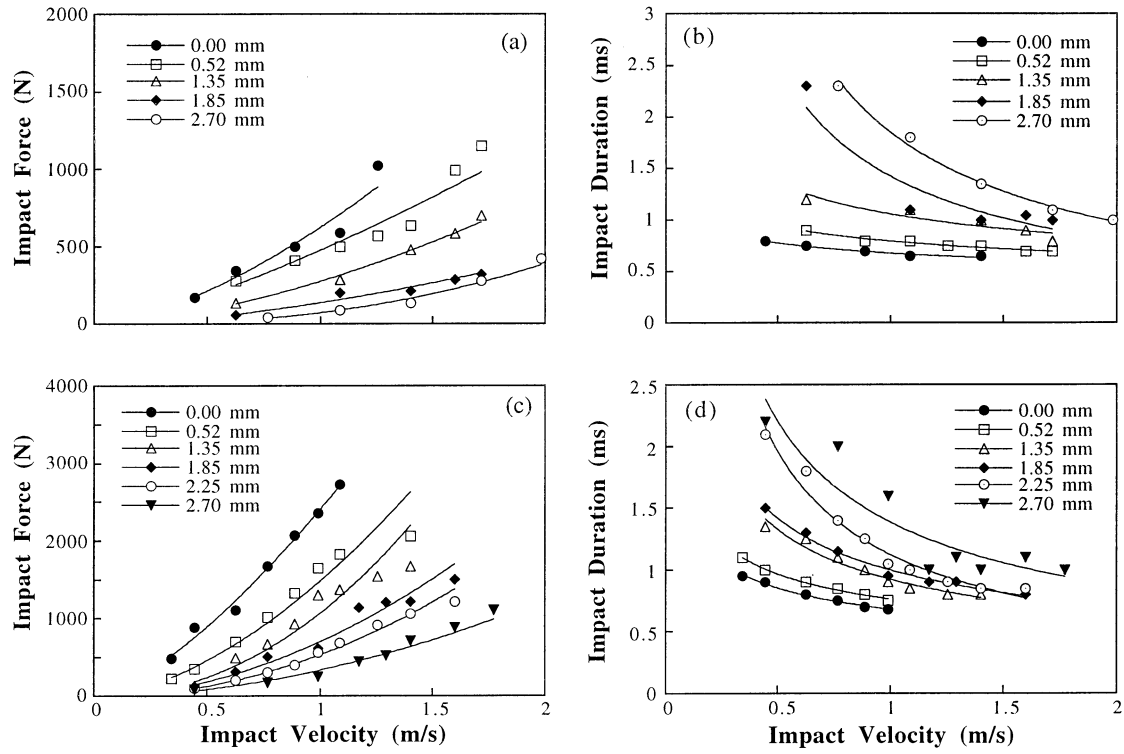


Fig. 6. Plots of the impact force as a function of the impact velocity for two different ball diameters of 38.2 mm: (a) magnitude and (b) duration, and of 50 mm: (c) magnitude and (d) duration.

$$\begin{cases} F \sim k^{-0.4} R^2 v^{1.2} \\ t \sim k^{0.4} R v^{-0.2} \end{cases} \quad (2)$$

where  $k$  is a constant related to the materials properties of the ball and plate,  $R$  is the radius of the ball and  $v$  is the impact velocity at the beginning of impact. As can be seen in Eq. (2), the velocity indices for both the force magnitude and duration are 1.2 and  $-0.2$ , respectively. The discrepancy between the experimental measurements of  $n_1$  and  $n_2$  and Hertz impact theory appears to be due to the fact that, unlike Hertz impact theory which treats colliding objects as being elastic, the ball and the plate exhibit some degree of inelasticity. In fact, Johnson has

pointed out that most impacts between metallic bodies involve some inelastic deformation [18]. When powder is included in the collision, the degree of inelasticity during impact is further enhanced. As shown in Table 1, the absolute values of  $n_1$  and  $n_2$  show an increasing trend with increasing powder thickness.

### 3.2.2. Effect of ball size

In Fig. 7, the magnitude and duration of the impact force are plotted as a function of ball size for various impact velocities. For all impact velocities, the magnitude of the impact force increases with increasing ball size (see Fig. 7(a) and (c)). The impact duration increases slightly

Table 1  
Curve-fitting coefficients for the relationship between the impact force and impact velocity

Powder thickness (mm)	38.2 mm ball			50 mm ball		
	$n_1$	$n_2$	$R_c$	$n_1$	$n_2$	$R_c$
0.00	1.53	-0.23	0.98	1.42	-0.33	0.99
0.52	1.33	-0.25	0.99	1.69	-0.34	0.99
1.35	1.60	-0.36	0.98	2.13	-0.52	0.98
1.80	1.62	-0.82	0.98	1.89	-0.50	0.98
2.25	—	—	—	2.03	-0.79	0.98
2.70	2.37	-0.91	0.98	1.89	-0.67	0.98

$R_c$  is the correlation coefficient ranging from 0 to 1 ( $R_c = 1$  implies a perfect fit).

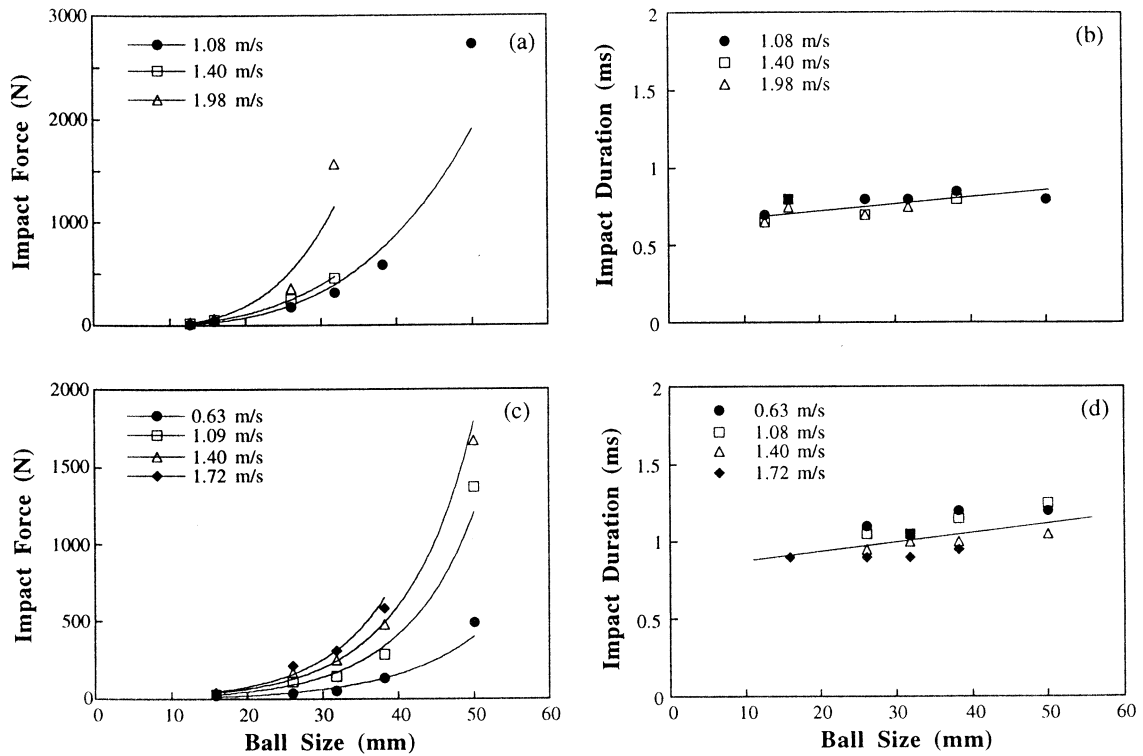


Fig. 7. Plots of the impact force as a function of the ball size for various powder thicknesses of 0 mm: (a) magnitude and (b) duration, and of 1.35 mm: (c) magnitude and (d) duration.

with increasing ball size (see Fig. 7(b) and (d)). A power law relationship,  $F \sim R^n$ , was also applied to fit the data in Fig. 7(a) and (c). Again, the fitted values of  $n$ , as shown in Table 2, are greater than that of the Hertz impact theory (where  $n = 2$ ) due to the inelasticity of the impacts. It can also be seen in Fig. 7(b) and (d) that the impact duration is approximately proportional to the ball size. However, the linear dependence of the impact duration on the ball size is significantly influenced by the powder thickness. The dependency becomes weaker as the powder thickness is increased.

3.2.3. Effect of powder thickness

The magnitude and duration of the impact force are

plotted as a function of powder thickness for various impact velocities and two different ball sizes in Fig. 8. It can be seen that for a fixed ball size and a fixed impact velocity, the magnitude of the impact force decreases (see Fig. 8(a) and (c)), while the duration increases (see Fig. 8(b) and (d)) as the powder thickness is increased.

The present results show that the impact between a ball and a plate is significantly influenced by the presence of powder. The deformation process of powder during an impact may be visualised in Fig. 9. When a ball with an initial velocity impacts the powder, the powder behaves as a porous material, as illustrated in Fig. 9(a). During the impact process, powder particles slide and rotate, rearranging their positions due to the particle interac-

Table 2  
Curve-fitting results for the relationship between the impact force and ball size

Impact velocity (m s <sup>-1</sup> )	No powder		Impact velocity (m s <sup>-1</sup> )	Powder thickness 1.35 mm	
	<i>n</i>	<i>R<sub>c</sub></i>		<i>n</i>	<i>R<sub>c</sub></i>
1.09	2.84	0.97	0.63	3.20	0.99
1.40	2.80	0.99	1.40	3.12	0.99
—	—	—	1.72	3.23	0.99
1.98	2.99	0.94	1.98	3.33	0.99

*R<sub>c</sub>* is the correlation coefficient ranging from 0 to 1 (*R<sub>c</sub>* = 1 implies a perfect fit).

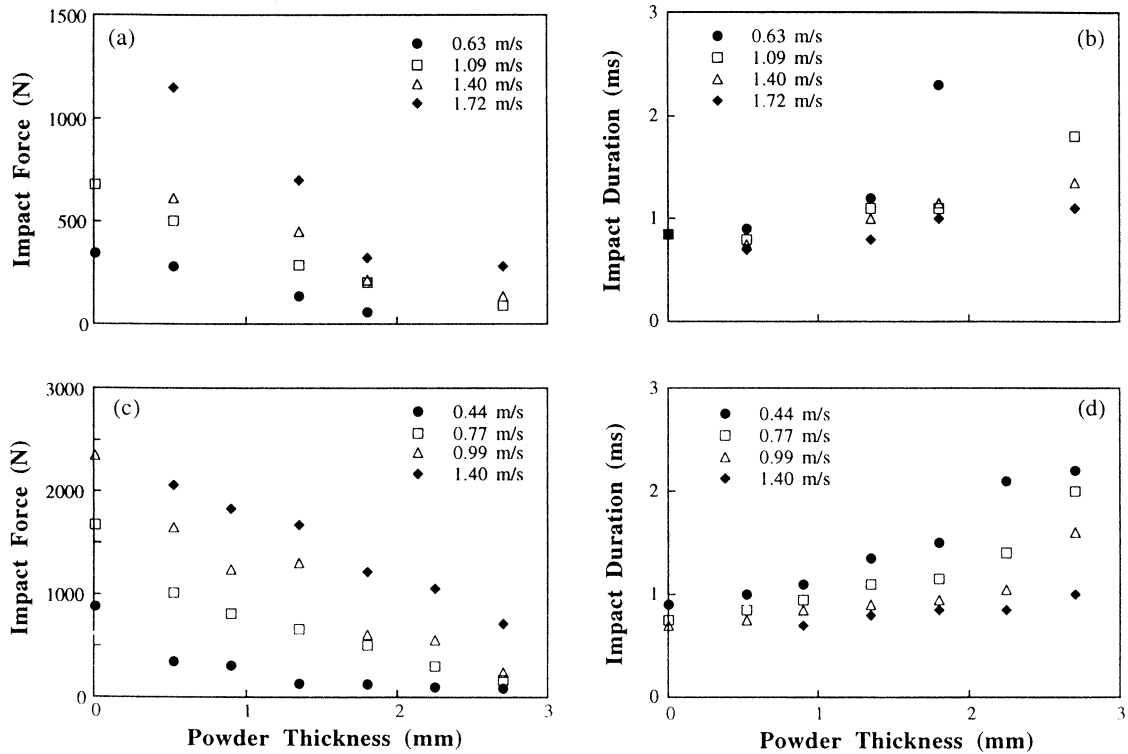


Fig. 8. Plots of the impact force as a function of the powder thickness for two different ball diameters of 38.2 mm: (a) magnitude and (b) duration, and of 50 mm: (c) magnitude and (d) duration.

tions. As a result, the porosity of the powder is decreased. Some of the particles may escape from the contact area. The porous structure of the powder will be altered with the progress of the impact until it is compressed to a critical height of  $h'$  (Fig. 9(b)). In this stage, a fraction of the kinetic energy of the ball is dissipated. The deformation associated with the collision could be dominated by the deformation of the porous structure of the powder. As the impact progresses further, the elastic and plastic deformation of the individual powder particles trapped in the contact area commences (Fig. 9(c)). The deformation of the ball and the plate during impact is relatively small compared with the deformation of the powder and thus may be neglected [18,22]. It is therefore inferred that when the powder is introduced to an impact, the impact duration is increased. As the impact force acting on an

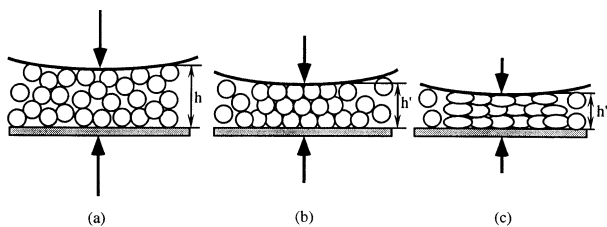


Fig. 9. Illustration of the deformation of powder during an impact process.

object is equal to the time rate of change of linear momentum, the thicker the powder, the longer the contact time and thus the smaller the magnitude of the impact force, and a decrease in the impact force then follows. This agrees with the experimental results presented above. The increase of the impact time and reduction in the impact force may be termed the ‘buffer’ effect of the powder.

3.2.4. Modelling impact forces

An improved understanding of mechanisms of impact characteristics can be gained by the development of realistic impact models. The results presented in this work clearly indicate that the effect of the presence of powder in

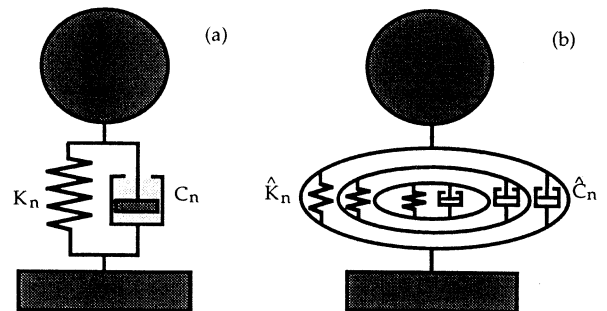


Fig. 10. Illustration of the model for describing the powder deformation: (a) the Kelvin model; and (b) the modified Kelvin model [26].

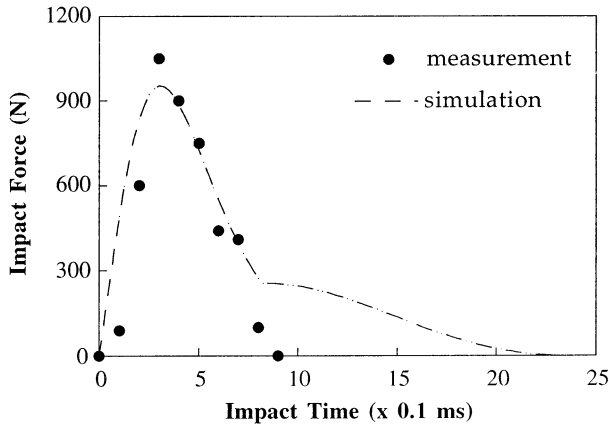


Fig. 11. Comparison of time histories of the impact force between experiment and simulation. Impact velocity  $0.99 \text{ m s}^{-1}$ , ball diameter 50 mm and powder thickness 0.52 mm.

the impact zone, which results in a high degree of inelasticity in the collision, must be included into such models.

The inelastic collision events during mechanical alloying have been previously modelled with the aid of a Kelvin viscoelastic couple [19,24,26]. As illustrated in Fig. 10(a), the conventional Kelvin model consists of a spring of stiffness  $K_n$  in parallel with a dashpot of viscoelastic resistance  $C_n$ . During an impact, energy absorbed by the dashpot is dissipated, thus simulating the plastic deformation of the powder. The normal impact force,  $F$ , is then the sum of the elastic and damping forces:

$$F = K_n \delta_n + C_n v_n \quad (3)$$

where  $\delta_n$  and  $v_n$  are the linear overlap and the relative velocity of approach of the colliding objects, respectively. Mishra and Rajamani [25] used the Kelvin model to simulate the inelastic collisions occurring in tumbling ball mills. Hashimoto et al. [24] have altered the Kelvin model to include spring and damping constants that vary with the linear overlap. This was done to more closely align the model with Hertz theory. Recently, Dallimore and McCormick [26] have modified the Kelvin model to reflect the impact dynamics likely to be present in the mechanical alloying process. In this model, the elastic force is proportional to the volume of the overlap,  $\delta_{vol}$ , while the damping force is proportional to both the velocity of approach and the instantaneous area of the impact,  $\delta_{area}$ . This impact model has been conceptualised as a system of concentric pairings of springs and dashpots in parallel, as shown in Fig. 10(b). Thus, the model incorporates some of the geometrical realities of impacts involving a spherical object and more closely resembles the local model of collisions in mechanical alloying proposed by Maurice and Courtney [27]. The impact force is now expressed as:

$$F = \hat{K}_n \delta_{vol} + \hat{C}_n v_n \delta_{area} \quad (4)$$

where  $\hat{K}_n$  and  $\hat{C}_n$  denote the modified spring and dashpot coefficients, having units of  $\text{N m}^{-3}$  and  $\text{N} \cdot \text{s m}^{-3}$ , respectively. The modified model has been shown to more closely follow the observed history, due to the fact that the Kelvin model predicts that the maximum force will occur in the first instant of a typical impact event during mechanical alloying [26]. This occurs due to the relatively large values of the damping and spring coefficients that must be specified in order to make the model accurately predict the value of the coefficient of restitution and reflect the estimated impact duration. The modified Kelvin model proposed by Dallimore and McCormick [26] was applied to predict the impact force and the coefficient of restitution.

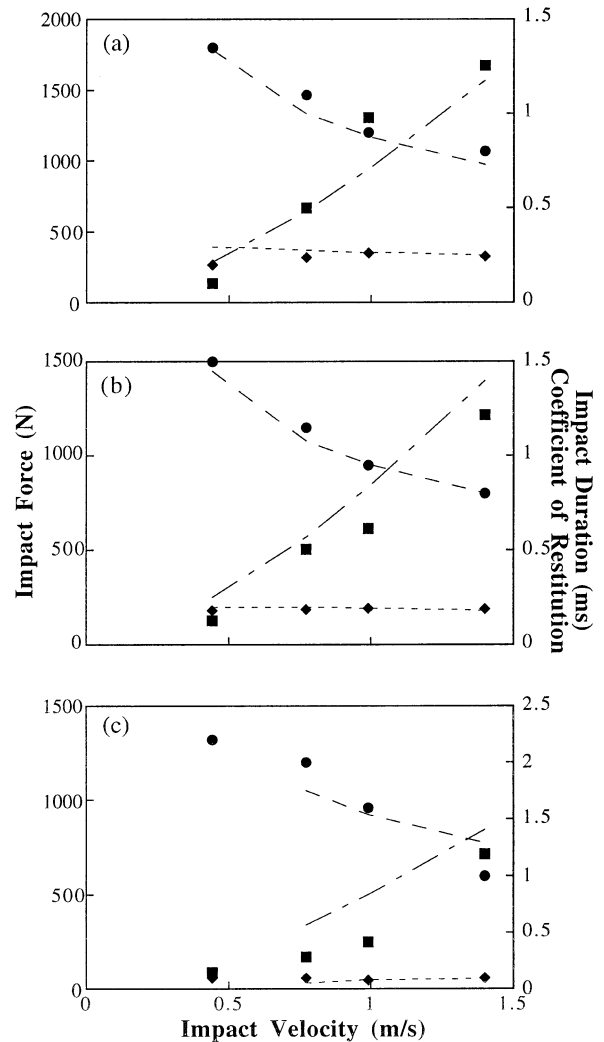


Fig. 12. Comparisons of the coefficient of restitution, and the magnitude and duration of the impact force between the measurement and prediction for ball size of 50 mm for various powder thicknesses of: (a) 0.52 mm; (b) 1.85 mm; and (c) 2.7 mm. (■ - - -) Magnitude of impact force; (● - - -) impact duration; (◆ - - -) coefficient of restitution.

A two-dimensional discrete element method (DEM) has been used to simulate the impact process of the free fall experiment. This method was developed by Cundall and Strack [28] and simply predicts a displacement time history for a system of distinct elements over a series of small time steps by a forward integrating procedure. For the free fall simulation only two elements are present, the rigidly mounted impact plate, which is assumed not to move during the impact, and the ball. The presence of the powder is accounted for in the modified Kelvin impact model. The simulation therefore calculates the motion of the ball from the release point, to just after the impact. A complete description of the DEM can be found elsewhere [26].

The simulation has been used to evaluate spring and dashpot coefficients for the different powder thicknesses and ball sizes of the free fall experiments. This has been done by iteratively altering the values of the coefficients until the simulation predicts the measured value of  $e$  as well as the point of the maximum force during an impact. A diagram showing an example of the fitted simulation force history against the measured results can be seen in Fig. 11. Here it can be seen that the initial peak of the impact model closely matches the measured response. The peak occurs during the approach of the ball and plate and is dominated by the damping component of the system. Note that the predicted tailing off in the impact force that occurs during the separation of impact objects cannot be matched to the measured force due to the presence of reflected stress waves in the experimental rig that are generated by the impact. Their effect upon the output of the force transducer is clearly visible in Fig. 2.

The predicted impact force and coefficient of restitution are shown in Figs. 12 and 13, together with the experimental results for two different ball sizes. The agreement between the prediction and measurement is reasonably good, particularly for the smaller powder thicknesses. There are some discrepancies in the magnitude of the impact force. The discrepancy becomes larger as the powder thickness is increased (Fig. 12(b) and (c), Fig. 13(c)). In Dallimore and McCormick's model, the impact force depends on the kinematically determined contact area and volume of the overlap. The influence of escaping powder during an impact is not included. It is expected that as the powder thickness is increased, the influence of the escaped powder on the impact process is enhanced, thus reducing the accuracy of the model. In addition, the experimental error (as we can see some outliers in Figs. 12 and 13) could also result in discrepancies between the prediction and the measurement. Experimental error is unavoidable due to the limited accuracy of the measurement and the complexity of the impact system. However, the effect of the outliers can be eliminated from a large number of repeated experiments. Future study should be carried

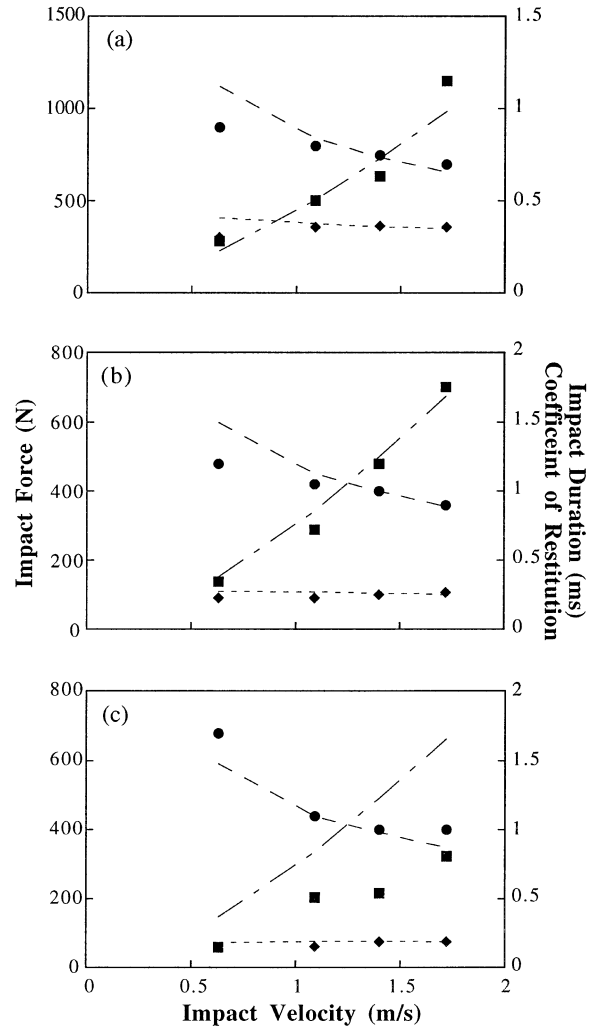


Fig. 13. Comparisons of the coefficient of restitution, and the magnitude and duration of the impact force between the measurement and prediction for ball size of 38.2 mm for various powder thicknesses of: (a) 0.52 mm; (b) 1.35 mm; and (c) 1.85 mm. (■ — —) Magnitude of impact force; (● - - -) impact duration; (◆ - - -) coefficient of restitution.

out using the statistical results from a large number of repeated experiments.

In Fig. 14, the spring and damping coefficients used in the computation are plotted as a function of powder thickness for two ball sizes of 50 and 38 mm. As expected, both the coefficients decrease with the increasing powder thickness. As the powder thickness is increased, the contact area and volume of the overlap is significantly increased. This produces smaller elastic and damping coefficients. When the powder thickness is sufficiently great, the spring coefficient tends towards zero, indicating that all the energy is dissipated in the interaction of powder particles. In other words, the powder behaves like a porous media during the whole

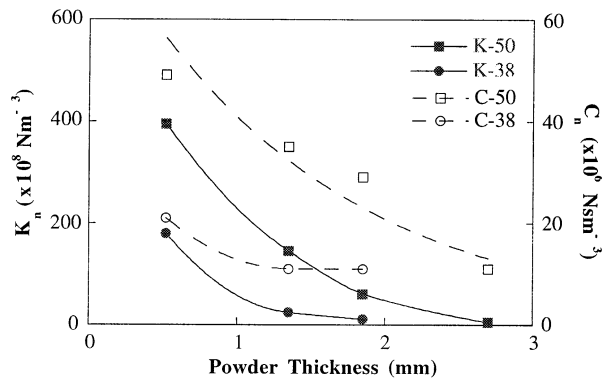


Fig. 14. Elastic and damping coefficients as a function of the powder thickness.

process and little deformation of the individual powder particles occurs. This evidence can be seen in Fig. 12(c), where for the powder thickness of 2.7 mm and an impact velocity of  $0.44 \text{ m s}^{-1}$ , the model predicted a perfectly inelastic collision. It should be noted that the larger powder thicknesses used in this investigation are only to show the likely extent of influence of the powder on the impact force. Provided that the powder does not experience any plastic deformation due to the large powder thickness, it is meaningless for mechanical alloying. It can also be seen from Fig. 14 that the values of both the coefficients for the 50 mm ball are greater than the respective values for the 38 mm ball. For given impact conditions, a larger ball, which has a larger mass, produces a more severe impact, thus resulting in larger values of both the coefficients.

#### 4. Concluding remarks

This investigation has illustrated that the free falling experiment provides a valuable tool for the evaluation of the effect of milling conditions on the impact characteristics involved in the mechanical alloying process. The impact force has been found to be an important parameter to evaluate the severity of the impact due to its sensitivity to milling conditions, such as the impact velocity, ball size and powder thickness. It has been shown that the impacts are significantly influenced by the presence of powder, necessitating the use of methods other than the Hertz impact theory to characterise the individual impact events.

The influence of the powder on the impact process is reflected mainly through the 'buffer' effect caused by its porous structure. When the powder thickness is increased, the 'buffer' effect of the powder is enhanced, thus resulting in a decrease in the magnitude of the impact force and an increase in the impact duration. This effect has been demonstrated using the

modified Kelvin model by changing the elastic and viscoelastic coefficients. The measurement and prediction of the impact force, the impact duration and the coefficients of restitution are in a reasonable agreement, particularly for smaller powder thicknesses. The larger discrepancies between the prediction and the measurement for larger powder thicknesses have been attributed to the limitations of the model.

#### References

- [1] C.C. Koch, in: R.W. Cahn, P. Haasen, E.J. Kramer (Eds.), *Materials Science and Technology*, VCH, Weinheim, 1991, pp. 193–246.
- [2] R.B. Schwarz, *Scr. Mater.* 34 (1996) 1–4.
- [3] D.R. Maurice, T.H. Courtney, *Metall. Trans. A* 21 (1990) 289–303.
- [4] F. Padella, E. Paradiso, N. Burgio, M. Magini, S. Martelli, W. Guo, A. Iasonna, *J. Less-Common Met.* 175 (1991) 79–90.
- [5] P.G. McCormick, H. Huang, M.P. Dallimore, J. Ding, J. Pan, in: *Proc. 2nd Int. Conf. Structural Application of Mechanical Alloying*, Vancouver, Canada, 20–22 September, 1993, pp. 45–50.
- [6] R.M. Davis, B. McDermott, C.C. Koch, *Metall. Trans. A* 19 (1988) 2867–2874.
- [7] E. Gaffet, *Mater. Sci. Eng. A* 119 (1989) 185–197.
- [8] E. Gaffet, L. Yousfi, *Mater. Sci. Forum* 88–90 (1992) 51–58.
- [9] M. Abdellaoui, E. Gaffet, *Acta Mater.* 44 (1996) 725–734.
- [10] M. Abdellaoui, E. Gaffet, *Acta Mater.* 43 (1995) 1087–1098.
- [11] Y. Chen, R. Le Hazif, G. Martin, *Mater. Sci. Forum* 88–90 (1992) 35–42.
- [12] H. Huang, J. Pan, P.G. McCormick, *Mater. Sci. Eng. A* (1997) in press.
- [13] H. Huang, J. Ding, P.G. McCormick, *Mater. Sci. Eng. A* 216 (1996) 178–184.
- [14] C. Zener, *Phys. Rev.* 59 (1941) 669–673.
- [15] S.P. Timoshenko, J.N. Goodier, *Theory of Elasticity*, McGraw-Hill, New York, 1970, pp. 409–414.
- [16] J.F. Doyle, *J. Sound Vib.* 118 (1987) 441–448.
- [17] R. Sondergaard, K. Chaney, C.E. Brennen, *J. Appl. Mech., Trans. ASME* 57 (1990) 694–699.
- [18] K.L. Johnson, *Contact Mechanics*, Cambridge University Press, Cambridge, UK, 1985, pp. 361–369.
- [19] K.N. Shivakumar, W. Elber, W. Illg, *J. Appl. Mech.* 52 (1985) 674–680.
- [20] I.H. Choi, C.S. Hong, *AIAA J.* 32 (1994) 2067–2072.
- [21] W.C. Jackson, C.C. Poe, *J. Comp. Tech. Res.* 15 (1993) 282–289.
- [22] G. Liang, E. Wang, H. Xian, *Scr. Metall. Mater.* 32 (1995) 451–455.
- [23] J.L. Meriam, L.G. Kraige, *Dynamics*, Wiley, New York, 1987, pp. 198–201.
- [24] H. Hashimoto, G. Geun Lee, R. Watanabe, *Mater. Trans., JIM* 35 (1994) 40.
- [25] B.K. Mishra, R.K. Rajamani, *KONA Powder Particle* 8 (1990) 92.
- [26] M.P. Dallimore, P.G. McCormick, *Mater. Trans., JIM* 37 (1996) 1091–1098.
- [27] D.R. Maurice, T.H. Courtney, *Metall. Trans. A* 25 (1994) 147–158.
- [28] P.A. Cundall, O.D.L. Strack, *Geotechnique* 29 (1979) 47–65.